Solid Earth Discuss., 2, 105–144, 2010
www.solid-earth-discuss.net/2/105/2010/

Solid Earth Discussions

This discussion paper is/has been under review for the journal Solid Earth (SE).
Please refer to the corresponding final paper in SE if available.

The mechanics of gravity-driven faulting

L. Barrows and V. Barrows

private address: 103 Gilmore Circle, Covington, LA 70433, USA

Received: 30 March 2010 – Accepted: 3 April 2010 – Published: 12 April 2010

Correspondence to: V. Barrows (vjbarrows@loopllc.com)

Published by Copernicus Publications on behalf of the European Geosciences Union.

Abstract

Faulting can result from either of two different mechanisms. These involve fundamentally different energetics. In elastic rebound, locked-in elastic strain energy is transformed into the earthquake (seismic waves plus work done in the fault zone). In force-driven faulting, the forces that create the stress on the fault supply work or energy to the faulting process. Half of this energy is transformed into the earthquake and half goes into an increase in locked-in elastic strain. In elastic rebound the locked-in elastic strain drives slip on the fault. In force-driven faulting it stops slip on the fault.

Tectonic stress is reasonably attributed to gravity acting on topography and the Earth's lateral density variations. This includes the thermal convection that ultimately drives plate tectonics. Mechanical analysis has shown the intensity of the gravitational tectonic stress that is associated with the regional topography and lateral density variations that actually exist is comparable with the stress drops that are commonly associated with tectonic earthquakes; both are in the range of tens of bar to several hundred bar.

The gravity collapse seismic mechanism assumes the fault fails and slips in direct response to the gravitational tectonic stress. Gravity collapse is an example of force-driven faulting. In the simplest case, energy that is released from the gravitational potential of the stress-causing topography and lateral density variations is equally split between the earthquake and the increase in locked-in elastic strain.

The release of gravitational potential energy requires a change in the Earth's density distribution. Gravitational body forces are solely dependent on density so a change in the density distribution requires a change in the body forces. This implies the existence of volumetric body-force displacements. The volumetric body-force displacements are in addition to displacements generated by slip on the fault. They must exist if gravity participates in the energetics of the faulting process.

From the perspective of gravitational tectonics, the gravity collapse mechanism is direct and simple. The related mechanics are more subtle. If gravity is not deliberately

and explicitly included in an earthquake model, then gravity is locked out of the energetics of the model. The earthquake model (but not necessarily the physical reality) is then elastic rebound.

1 Introduction

A tectonically active Earth is clearly demonstrated by sheared metamorphic rock fabrics, faulted and deformed geologic strata, epeirogenic uplift and subsidence, global plate tectonics, and earthquakes. These features and phenomena result from tectonic stress that acts to deform the materials. The basic premise of gravitational tectonics is that most; and quite possibly all; tectonic stress originates from gravity acting on the Earth's topography and lateral density variations. This conclusion follows from the ability of gravity to explain most tectonic processes and the lack of alternate mechanisms that can produce large shear stresses that are capable of acting through large deformations. Some processes such as thermal expansion can create large stresses but these are entirely relaxed by relatively small deformations. Other processes such as solar and lunar tides can act through large deformations but their intensity is relatively small. Only gravity appears capable of producing the tectonic features that actually exist.

Through a combination of scaled centrifuge models and mechanical analysis, Romberg (1981) demonstrated how gravity produces diapers, deformed strata, and many of the structures found in mountain belts. Jacoby (1970) demonstrated how the gravity driven rise of hot low-density material in spreading centers and complimentary sinking of cool high-density material in subduction zones can drive global plate tectonics. Our current understanding of this push-from-the-ridge plus pull-from-the-trench plate tectonic driving mechanism is described in Stein and Wysession (2003, Sect. 5). DeJong and Scholten (1973) provide a compendium of articles relating specific geologic features to gravitational tectonics. The comprehensive scope of gravitational tectonics is evident in the range of features described. Artyushkov

(1973) showed the deviatoric stress associated with isostatically-compensated sinusoidal variations in regional topography is comparable with the vertical load of the excess topography – at 2.5 gm/cc this equals 245 bar per kilometer of topographic relief (10 bar = 1 megaPascel). Ruff (2002) reviews our current understanding of the origin of tectonic stress and the state of stress within the Earth; again it is recognized that gravity acting on topography and density variations is the primary source of tectonic stress and shear stresses of several hundred bar are associated with the regional topography and lateral density variations that actually exist.

Topography, lateral density variations, and stratified density inversions increase the gravitational potential energy of the Earth above that which would exist if the same materials were arranged in smooth concentric layers with the less dense material on top. Gravitational tectonic stress drives the configuration towards the lower energy state. Other processes such as thermal expansion and contraction, mineral phase change, glaciation, or erosion and deposition can create the topography and density variations – but the stress results from gravity. Ultimately included in this broad tectonic paradigm are tectonic earthquakes.

Earthquakes have traditionally been assumed to result from elastic rebound. In the elastic rebound mechanism, locked-in elastic strain energy that previously accumulated through slow tectonic deformation is released from the epicentral volume and at least partially transformed into seismic waves. This model was based on the observation that the 1906 San Francisco Earthquake was accompanied by a change in elastic strain energy that approximately equaled the seismic wave energy (Reid, 1910). We should note that the observations did not determine if the co-seismic change in locked-in elastic strain energy was a decrease or an increase. The models in the Appendix show this distinction can be of primary importance to the earthquake mechanics.

An alternate (and largely unexplored) gravity-collapse mechanism assumes the earthquake fault fails and slips in direct response to the gravitational tectonic stress. Gravity collapse is similar to elastic rebound in that both mechanisms involve stress driven slip on the fault and a change in locked-in elastic strain energy whose absolute

magnitude equals the earthquake energy. The gravity collapse mechanism differs in that the change in elastic strain energy is an increase and both the earthquake energy and the increase in elastic strain energy come from a decrease in the gravitational potential energy of the stress-causing density structures. In elastic rebound the locked-in elastic stress drives slip on the fault. In gravity collapse it stops slip on the fault.

Barrows and Langer (1981) demonstrate the gravity-collapse mechanism with a finite-element model of a gravity-driven high-angle thrust fault in the lowlands adjacent to an isostatically-compensated increase in regional elevation. They also note the land surface topographic deformation that accompanied the 1964 Good Friday Earthquake in Alaska involved a decrease in gravitational potential energy that was comparable to the seismic wave energy. Barrows and Paul (1998) show the intensity of the shear stress associated with simple density models of a plate-tectonic spreading center and a subduction zone is several tens of bar to over 100 bar. This shear stress intensity is comparable to the stress drops commonly associated with tectonic earthquakes (e.g. Kasahara, 1981, Fig. 6.7). An important implication of this equivalency is gravitational tectonic stress can directly drive earthquakes in these environments. It is noted the shear stress component of the total gravitational stress results from lateral density variations. Vertical density stratification affects the lithostatic pressure component of the total stress but not the shear stress. Barrows and Paul also show a strong coincidence between the shear stress intensity in the model of a gravity-driven subducted plate and the dual-plane seismicity in the Wadati-Benioff zone beneath Honshu, Japan. Barrows (2008) explains how the lithostatic pressure component of the total stress is balanced by locked-in pressure in the solid rocks of the Earth.

The mechanics of faulting need to be understood if the gravity collapse mechanism is to be appreciated. Faulting and earthquakes can result from either of two different mechanisms. In *elastic rebound* locked-in elastic strain energy is transformed into the earthquake. In *force-driven faulting* work or energy is supplied by the forces that created the shear stress on the fault surface. Half of this energy is transformed into the earthquake and half goes into an increase in locked-in elastic strain. Gravity collapse is

an example of force-driven faulting. The Appendix provides finite-element models that demonstrate the similarities and differences between elastic rebound and force-driven faulting.

In the current paper, the gravity collapse mechanism is explored through:

- A couple of simple conceptual models,
- The finite-element equations for force-driven faulting, and
- The potential-field relations between gravitational potential energy, density, and body forces.

It is shown that volumetric body–force displacements must accompany a gravity collapse event. These are in addition to the displacements generated by slip on the fault surface; they originate from throughout the volume in which the density structure changes. If the volumetric body–force displacements are not explicitly included in an earthquake model, then gravity is locked out of the energetics of the model.

2 Models

2.1 Spring-mass oscillator

The energetics of partial spring failure in a spring-mass oscillator (Fig. 1) closely resemble the energetics of gravity-driven faulting in a three-dimensional body. They are reviewed here to provide insight into the energetics of the more complicated systems.

Static equilibrium is expressed as:

$$ku = F \tag{1}$$

Where: k is the spring stiffness, u is the spring extension, and $F = Mg$ is the weight of the mass.

The elastic strain energy in the spring is

$$\mathrm{SE}=\frac{1}{2}ku^2=\frac{1}{2}\frac{F^2}{k} \tag{2}$$

The gravitational potential energy can be expressed as

$$\mathrm{GP}=-Fu=-\frac{F^2}{k} \tag{3}$$

The spring stiffness can be regarded as the supporting structure in a gravity-loaded mechanical system. Consider what happens if part of this supporting structure fails. This can be simulated by an instantaneous reduction in the spring stiffness.

$$k_{(\mathrm{f})} = k_{(\mathrm{i})} - \Delta k \tag{4}$$

Where: $k_{(\mathrm{f})}$ is the final spring stiffness, $k_{(\mathrm{i})}$ is the initial spring stiffness, and Δk is the change in the spring stiffness.

There is an increase in the elastic strain energy

$$\Delta\mathrm{SE}=\mathrm{SE}_{(\mathrm{f})}-\mathrm{SE}_{(\mathrm{i})}$$

$$\Delta\mathrm{SE}=\frac{1}{2}F^2\left\langle\frac{1}{k_{(\mathrm{f})}}-\frac{1}{k_{(\mathrm{i})}}\right\rangle \tag{5}$$

And a decrease in gravitational potential energy

$$\Delta\mathrm{GP}=\mathrm{GP}_{(\mathrm{f})}-\mathrm{GP}_{(\mathrm{i})}$$

$$\Delta\mathrm{GP}=-F^2\left\langle\frac{1}{k_{(\mathrm{f})}}-\frac{1}{k_{(\mathrm{i})}}\right\rangle \tag{6}$$

Equations (5) and (6) show the increase in elastic strain energy is one-half as large as the decrease in gravitational potential energy.

The change in the static spring extension is

$$\Delta u = u_{(\mathrm{f})} - u_{(\mathrm{i})} \tag{7}$$

The energy of the oscillations that are induced in the spring-mass system is

$$\mathrm{EQ}=\frac{1}{2}k_{(\mathrm{f})}\Delta u^2 \tag{8}$$

$$\mathrm{EQ}=\frac{1}{2}k_{(\mathrm{f})}\left\langle u_{(\mathrm{f})}^2-2\,u_{(\mathrm{f})}\,u_{(\mathrm{i})}+u_{(\mathrm{i})}^2\right\rangle$$

$$\mathrm{EQ}=\frac{1}{2}k_{(\mathrm{f})}\left\langle\frac{F^2}{k_{(\mathrm{f})}^2}-2\frac{F^2}{k_{(\mathrm{f})}k_{(\mathrm{i})}}+\frac{F^2}{k_{(\mathrm{i})}^2}\right\rangle$$

$$\mathrm{EQ}=\frac{1}{2}F^2\left\langle\frac{1}{k_{(\mathrm{f})}}-\frac{2}{k_{(\mathrm{i})}}+\frac{k_{(\mathrm{i})}-\Delta k}{k_{(\mathrm{i})}^2}\right\rangle$$

$$\mathrm{EQ}=\frac{1}{2}F^2\left\langle\frac{1}{k_{(\mathrm{f})}}-\frac{1}{k_{(\mathrm{i})}}\right\rangle-\frac{1}{2}\Delta k\frac{F^2}{k_{(\mathrm{i})}^2}$$

$$\mathrm{EQ}=\frac{1}{2}F^2\left\langle\frac{1}{k_{(\mathrm{f})}}-\frac{1}{k_{(\mathrm{i})}}\right\rangle-\frac{1}{2}\Delta k u_{(\mathrm{i})}^2 \tag{9}$$

The first term in Eq. (9) equals the difference between the decrease in gravitational potential energy and the increase in elastic strain energy. The second term is the elastic strain energy that was initially stored in that part of the mechanical structure that failed.

These mechanics can be demonstrated with a small rock suspended from a rigid support by a cluster of three or four very-long rubber bands. With the system in static

equilibrium, cut one of the rubber bands with a pair of scissors. The rock drops to a lower position releasing gravitational potential energy (Eq. 6), the remaining rubber bands are further stretched increasing the elastic strain energy (Eq. 5), and the rock spontaneously oscillates about its new equilibrium position (Eq. 9). The second term in Eq. (9) is the elastic strain energy that was initially stored in the rubber band that was cut. It is shown below that similar mechanics apply to gravity-driven earthquakes in three dimensional bodies.

2.2 Conceptual models: elastic rebound and force-driven faulting

Below are the contrasting energetics of elastic rebound and force-driven faulting. They are first discussed through conceptual models. The energetics of force-driven faulting are then explored through the general equations of a finite-element model. The Appendix to this report describes plane-strain finite-element computer simulations of the conceptual models.

2.2.1 Elastic rebound

Consider a solid block of elastic material enclosed in a rigid frame. Distort the rigid frame creating locked-in elastic stress and strain. In Fig. 2a this is shown as the maximum and minimum principal stresses associated with a simple shear deformation. The intermediate principal stress is perpendicular to the plane of the figure.

Let a fault fail and slip in direct response to the locked-in stress (Fig. 2b). In the simplest approximation, fault failure could be simulated as a sudden decrease in the shear strength of the fault; the initial shear strength would correspond to static friction between the sides of the fault and the final shear strength would correspond to dynamic or sliding friction. The resulting static and dynamic displacements are attributable to slip on the fault. The earthquake energy equals the decrease in locked-in elastic strain energy and the locked-in stress drives slip on the fault. The mechanics are those of the elastic rebound mechanism. Figure 2 is comparable to the figures that have traditionally

been used to illustrate elastic rebound (e.g. Bolt, 2004, p. 89; Hough, 2002, p. 27; Stein and Wysession, 2003, p. 216). When considering elastic rebound, it is appropriate to question the geologic nature of the “rigid frame” that isolates the elastic material in the epicentral volume from the forces that drive the larger tectonic deformation.

2.2.2 Force-driven faulting

Now consider the same block of elastic material loaded by constant forces (Fig. 3a). In the current example, the forces are shown as surface tractions but they could just as well be point loads or gravitational body forces. By judiciously selecting the forces, the stress and strain are identical to those in the model of elastic rebound (Sect. 2.2.1). In the force-loaded model the stress results directly from the forces and is not locked into the structure. As before, let a fault fail and slip in direct response to the stress (Fig. 3b). The process is similar to elastic rebound but; as explained below and demonstrated in the Appendix; the energetics are not.

When the fault fails, the block temporarily becomes less rigid than it was before the fault failed. During this interval, the same forces are acting on a less rigid block so there is additional deformation of the block. These force-connected displacements are in addition to the displacements generated by slip on the fault.

Along the sides of the block, the force-connected displacements parallel the forces and the scalar or dot product of force and displacement equals work or energy. Through this connection, the forces that created the stress on the fault provide energy to the earthquake. Note that if the force-connected displacements are assumed to be zero or not included in the model, the forces are precluded from participating in the energetics. The model is then identical to the model of elastic rebound described in Sect. 2.2.1. Force-connected displacements are an essential part of the mechanics and energetics of force-driven faulting.

We should further consider the role of locked-in stress and strain. In elastic rebound, fault slip will relax the locked-in shear stress that was acting on the fault – this is the stress drop. In force-driven faulting, slip on the fault will also relax the shear stress on

the fault surface. But in the post-faulting environment the same forces are acting on the block. In the absence of locked-in strain, these forces would produce the stress field shown in Fig. 3a. The only way to have a post-seismic fault zone with negligible remaining shear stress is to balance the force-induced stress on the fault with a locked-in elastic stress on the fault. This locked-in stress is created at the time of the earthquake. In elastic rebound, the locked-in elastic stress drives slip on the fault. In force-driven faulting, it stops slip on the fault.

Another perspective on the locked-in stress follows from consideration of mechanical equilibrium. If the forces acting on the block are constant, the net resistance offered by the block must also be constant. When the fault failed, that part of the net force that was supported by the fault will be redistributed into the remainder of the block. After the earthquake, when the fault surface reverts back to static friction, the redistributed force becomes an anomalous locked-in stress field.

2.3 Energetics

The energetics of force-driven faulting can be explored through the equilibrium equations for a finite element model. In a finite element model, the continuous material is subdivided into a two-dimensional assemblage of triangular elements or a three-dimensional assemblage of tetrahedral elements each defined by three (triangular elements) or four (tetrahedral elements) nodal points. Material displacements are assumed to vary in a linear fashion between the nodes of each element; the nodal point displacements are the unknowns in the problem. Surface tractions, applied loads, and gravitational body forces are resolved into equivalent forces applied at the nodes. In the limit as the number of nodal points becomes large and the size of the elements becomes small, the solution to a finite element model approaches the exact solution to the continuous, linear-elastic, boundary value problem.

Desai and Able (1972), Zienkiewicz (1971), and other engineering texts describe finite-element modeling. Barrows and Paul (1998) describe applications of finite-element modeling to problems in gravitational tectonics.

Equilibrium within a simple force-loaded finite element model can be expressed as

$$[\mathbf{K}]\{\boldsymbol{U}\} = \{\boldsymbol{F}\} \tag{10}$$

Where: [**K**] is a large, symmetric, elastic stiffness matrix, $\{\boldsymbol{U}\}$ is a vector array of the unknown nodal displacements, and $\{\boldsymbol{F}\}$ is a vector array of the forces at the nodal points.

The solution is:

$$\{\boldsymbol{U}\} = \left[\mathbf{K}^{-1}\right]\{\boldsymbol{F}\} \tag{11}$$

Where $\left[\mathbf{K}^{-1}\right]$ is the inverse of the stiffness matrix.

The net static displacements due to faulting can be modeled by changing those elements of the stiffness matrix that represent the shear strength of the fault zone. The initial values would represent static friction between the two sides of the fault and the final values would represent dynamic or sliding friction. The static displacements due to faulting are the differences between the initial equilibrium displacements and the equilibrium displacements after modification of the stiffness matrix. The earthquake is the transformation between these two states of static equilibrium.

The change in the stiffness matrix is represented by:

$$\left[\mathbf{K}_{(\mathrm{f})}\right] = \left[\mathbf{K}_{(\mathrm{i})}\right] - [\boldsymbol{\Delta}\mathbf{K}] \tag{12}$$

Where: (i) and (f) refer to the initial and final states, and [**ΔK**] is a sparsely populated matrix of changes to the stiffness matrix.

The associated change in the equilibrium displacements is

$$\{\Delta\boldsymbol{U}\} = \left\langle \left[\mathbf{K}_{(\mathrm{f})}^{-1}\right] - \left[\mathbf{K}_{(\mathrm{i})}^{-1}\right] \right\rangle \{\boldsymbol{F}\} \tag{13}$$

The work done by the forces is

$$\Delta\mathrm{GP} = \{\boldsymbol{F}\}^{T}\{\Delta\boldsymbol{U}\} \tag{14}$$

$$\Delta GP = \{F\}^T \left\langle \left[\mathbf{K}_{(f)}^{-1}\right] - \left[\mathbf{K}_{(i)}^{-1}\right] \right\rangle \{F\} \quad (15)$$

Where $\{F\}^T$ is the transpose of the vector array of the nodal-point forces.

The change in the elastic strain energy is

$$\Delta SE = SE_{(f)} - SE_{(i)} \quad (16)$$

$$\Delta SE = \frac{1}{2}\{U_{(f)}\}^T [\mathbf{K}_{(f)}] \{U_{(f)}\} - \frac{1}{2}\{U_{(i)}\}^T [\mathbf{K}_{(i)}] \{U_{(i)}\}$$

$$\Delta SE = \frac{1}{2}\{F\}^T \left\langle \left[\mathbf{K}_{(f)}^{-1}\right] - \left[\mathbf{K}_{(i)}^{-1}\right] \right\rangle \{F\}. \quad (17)$$

Equations (15) and (17) indicate the change in elastic strain energy is an increase that is one-half as large as the work done by the forces.

At the instant the fault fails, the energy available for dynamic vibrations exists as displacements beyond the final equilibrium displacements. These are the initial peak amplitudes before the seismic waves and deformations propagate through the material. They also include the energy available to create the fault and drive slip on the fault surface. This energy is

$$EQ = \frac{1}{2}\{\Delta U\}^T [\mathbf{K}_{(f)}] \{\Delta U\} \quad (18)$$

Substituting:

$$\{\Delta U\}^T = \{F\}^T \left\langle \left[\mathbf{K}_{(f)}^{-1}\right]^T - \left[\mathbf{K}_{(i)}^{-1}\right]^T \right\rangle$$

$$\{\Delta U\} = \left\langle \left[\mathbf{K}_{(f)}^{-1}\right] - \left[\mathbf{K}_{(i)}^{-1}\right] \right\rangle \{F\}$$

And noting:

$\left[\mathbf{K}^{-1}\right][\mathbf{K}] = [I]$ the identity matrix,

$[\mathbf{K}]^T = [\mathbf{K}]$ the stiffness matrix (and its inverse) are symmetric,

$$\{U_{(i)}\} = \left[\mathbf{K}_{(i)}^{-1}\right] \{F\}$$

Then the earthquake energy can be reformatted as

$$EQ = \frac{1}{2}\{F\}^T \left\langle \left[\mathbf{K}_{(f)}^{-1}\right] - \left[\mathbf{K}_{(i)}^{-1}\right] \right\rangle \{F\} - \frac{1}{2}\{U_{(i)}\}^T [\Delta \mathbf{K}] \{U_{(i)}\} \quad (19)$$

The first term in Eq. (19) equals the difference between the work done by the forces and the increase in elastic strain energy. The second term is the elastic strain energy originally stored in the material that failed. For a planer fault zone, the volume of material in the fault zone is negligible and the energy in the second term is negligible.

In force-driven faulting, the forces that created the stress on the fault provide work or energy to the faulting process. The finite-element Eqs. (15), (17), (19) show half this work goes into an increase in elastic strain energy and half goes into seismic waves plus work done in the fault zone. The earthquake energy equals the change in elastic strain energy but the change in elastic strain energy is an increase and all of the energy comes from the work done by the forces. Below is a summary of these mechanics.

Elastic rebound:

- Energy is transformed from a locked-in elastic strain field into the earthquake,
- The change in locked-in elastic strain *drives* slip on the fault.

Force-driven faulting:

- Through the force-connected displacements, work (or energy) is provided by the forces that created the stress on the fault,
- Half of this energy is transformed into the earthquake and half goes into an increase in locked-in elastic strain,

– The change in locked-in elastic strain *stops* slip on the fault.

The finite element Eqs. (10), (11) do not differentiate between surface tractions, externally-applied loads, and body forces – all are resolved into equivalent forces applied at the nodes and all are added to the vector array of nodal point forces. For an isolated, self-gravitating elastic body that initially does not contain locked-in strain; the forces would be gravitational body forces. The work done by the forces would then come from the gravitational potential energy of the stress-causing density structures. The density structures exist as surface topography or lateral variations in rock density. The release of gravitational potential energy implies the stress-causing density structures move towards a lower-energy or more-flat configuration. For the Earth, the lowest energy configuration would be smooth concentric layers with the less dense material on top. A finite element model demonstrating these energetics is available in Barrows and Langer (1981).

This decrease in gravitation potential energy may have been directly observed in the 1964 Good Friday Earthquake in Alaska. The co-seismic vertical land surface deformation was evident in drowned forests, raised coastlines, tide-gage measurements, sea-floor depth soundings, first-order level lines, and the resulting tsunami (Plafker, 1972). These data showed that a large area centered on Kodiak Island and the Kenai Peninsula subsided, a corresponding area on the continental shelf and slope was uplifted. If we assume the area of subsidence was on average one kilometer above the area of uplift and the volume of uplift equaled the volume of subsidence, then the release of gravitational energy was 1.5×10^{25} ergs (Barrows and Langer, 1981). This is five times the 3×10^{24} ergs of seismic energy associated with the main shock (Press and Jackson, 1972). These energetics are consistent with the gravity-driven mélange wedge model of shallow low-angle thrust faulting in subducton zones (Hamilton, 1973; Dickinson, 1977).

3 Volumetric body-force displacements

3.1 Potential field relations

The release of gravitational potential energy requires a change in the density distribution. This rather obvious statement follows from the closed-form expression for the gravitational potential energy in an arbitrary density distribution (e.g. Kellogg, 1954).

$$\mathrm{GP} = -\frac{G}{2} \int_{V(\boldsymbol{x})} \int_{V(\boldsymbol{\eta})} \frac{\rho(\boldsymbol{x})\rho(\boldsymbol{\eta})}{|\boldsymbol{x}-\boldsymbol{\eta}|} dV(\boldsymbol{\eta}) dV(\boldsymbol{x}) \tag{20}$$

Where: GP is the gravitational potential energy, ρ is the density distribution, G is the gravitational constant, and $|\boldsymbol{x}-\boldsymbol{\eta}|$ is the absolute distance between position vectors $\boldsymbol{x}$ and $\boldsymbol{\eta}$.

The gravitational potential (not the gravitational potential energy) is a density-dependent mathematical construct equal to:

$$\Phi(\boldsymbol{x}) = -G \int_{V(\boldsymbol{\eta})} \frac{\rho(\boldsymbol{\eta})}{|\boldsymbol{x}-\boldsymbol{\eta}|} dV(\boldsymbol{\eta}) \tag{21}$$

The gravitational body force per unit volume equals the local density times the negative gradient of the gravitational potential, or

$$f_p(\boldsymbol{x}) = -\rho \frac{\partial \Phi}{\partial x_p} \tag{22}$$

Because the gravitational potential and the gravitational body force are solely dependent on the density distribution, a change in the density distribution requires a change in the body force field.

The elastic Green's tensor describes the time-dependent displacement at one location in a body due to a time-dependent unit force applied at a different location (e.g. Aki

and Richards, 1980). The elastic Green's tensor can be expressed as:

$$\Gamma_{np}(\boldsymbol{x},t;\boldsymbol{\eta},\tau) \tag{23}$$

Where: $(\boldsymbol{x},t)$ is location and time of the observation point, $(\boldsymbol{\eta},\tau)$ is location and time of the force, and $\Gamma_{np}(\boldsymbol{x},t;\boldsymbol{\eta},\tau)$ is the x_n component of displacement at $(\boldsymbol{x},t)$ due to an $x_p$directed unit force at $(\boldsymbol{\eta},\tau)$.

In terms of the Green's tensor, the x_n component of the displacements that would result from a change in the body force field can be expressed as:

$$\Delta u_n(\boldsymbol{x},t) = \int_{\infty} d\tau \int_{V(\boldsymbol{\eta})} \Delta f_p(\boldsymbol{\eta},\tau)\Gamma_{np}(\boldsymbol{x},t;\boldsymbol{\eta},\tau)dV(\boldsymbol{\eta}) \tag{24}$$

Where $\Delta f_p(\boldsymbol{\eta},\tau)$ is the x_p component of the change in the body force field, and the summation convention on repeated indices is in effect.

These volumetric body force displacements are in addition to the displacements generated by slip on the fault surface. The potential field relations show the volumetric body force displacements *must exist* if gravity is involved in the earthquake energetics.

3.2 Seismic source equations

The subtle importance of the volumetric body-force displacements can be explored through the seismic source equations. Aki and Richards provide a general expression for the displacements due to faulting in an isolated, self-gravitating, elastic body (1980, Sect. 3, Eq. 3-1). This expression contains three terms associated with body forces, slip on the fault, and surface tractions on the fault. It can be written as:

$$u_n(\boldsymbol{x},t) = \int_{\infty} d\tau \int_{V(\boldsymbol{\eta})} f_p(\boldsymbol{\eta},\tau)\Gamma_{np}(\boldsymbol{x},t;\boldsymbol{\eta},\tau)dV(\boldsymbol{\eta}) \qquad \leftarrow \text{Body Forces} \tag{25}$$

$$+\int_{\infty} d\tau \int_{\Sigma(\boldsymbol{\xi})} [u_i(\boldsymbol{\xi},\tau)]\upsilon_j c_{ijpq}\frac{\partial}{\partial \xi_q}\Gamma_{np}(\boldsymbol{x},t;\boldsymbol{\xi},\tau)d\Sigma(\boldsymbol{\xi}) \quad \leftarrow \text{Slip on the Fault} \tag{26}$$

$$+\int_{\infty} d\tau \int_{\Sigma(\boldsymbol{\xi})} \left[T_p(\boldsymbol{\xi},\tau,\hat{\upsilon})\right]\Gamma_{np}(\boldsymbol{x},t;\boldsymbol{\xi},\tau)d\Sigma(\boldsymbol{\xi}) \qquad \leftarrow \text{Surface Tractions} \tag{27}$$

Where: $f_p(\boldsymbol{\eta},\tau)$ is the x_p component of the body force at $(\boldsymbol{\eta},\tau)$, $\Gamma_{np}(\boldsymbol{x},t;\boldsymbol{\eta},\tau)$ is the elastic Green's Tensor, $[u_i(\boldsymbol{\xi},\tau)]$ is the x_i component of slip on the fault at $(\boldsymbol{\xi},\tau)$. The brackets indicate integration is over both sides of the fault, υ_j is a unit normal to the fault surface, c_{ijpq} is the heterogeneous anisotropic elasticity tensor, and $\left[T_p(\boldsymbol{\xi},\tau,\hat{\upsilon})\right]$ is surface traction parallel with the fault surface.

For an isolated body, surface tractions are balanced across the fault so the net surface traction term is zero. In the development of the moment tensor representation of the seismic source, Aki and Richards (p. 39) also assume the absence of body forces and drop the first term. Dropping the body-force term is consistent with the restrictive assumption that all displacements are generated solely by slip on the fault. We need to further consider the consequences of this assumption.

Without the surface traction and body-force terms, the displacement field is:

$$u_n(\boldsymbol{x},t) = \int_{\infty} d\tau \int_{\Sigma(\boldsymbol{\xi})} [u_i(\boldsymbol{\xi},\tau)]\upsilon_j c_{ijpq}\frac{\partial}{\partial \xi_q}\Gamma_{np}(\boldsymbol{x},t;\boldsymbol{\xi},\tau)d\Sigma(\boldsymbol{\xi}) \tag{28}$$

The associated net change in gravitational potential energy equals the integrated scalar product of the gravitational body force field and the displacement field.

$$\Delta\text{GP} = -\int_{\infty} dt \int_{V(\boldsymbol{x})} f_n(\boldsymbol{x},t)u_n(\boldsymbol{x},t)dV(\boldsymbol{x}) \tag{29}$$

Substitute Eq. (28) for $u_n(\boldsymbol{x},t)$

$$\Delta\text{GP} = -\int_{\infty} dt \int_{V(\boldsymbol{x})} f_n(\boldsymbol{x},t)\int_{\infty} d\tau \int_{\Sigma(\boldsymbol{\xi})} [u_i(\boldsymbol{\xi},\tau)]\upsilon_j c_{ijpq}\frac{\partial}{\partial \xi_q}\Gamma_{np}(\boldsymbol{x},t;\boldsymbol{\xi},\tau)d\Sigma(\boldsymbol{\xi})dV(\boldsymbol{x}) \tag{30}$$

Rearrange the order of integration

$$\Delta GP = -\int_{\infty}^{} d\tau \int_{\Sigma(\boldsymbol{\xi})} [u_i(\boldsymbol{\xi},\tau)] \upsilon_j c_{ijpq} \frac{\partial}{\partial \xi_q} \int_{\infty}^{} dt \int_{V(\boldsymbol{x})} f_n(\boldsymbol{x},t) \Gamma_{np}(\boldsymbol{x},t;\boldsymbol{\xi},\tau)\, dV(\boldsymbol{x})\, d\Sigma(\boldsymbol{\xi}) \tag{31}$$

Note the reciprocity of the Green's tensor

$$\Gamma_{np}(\boldsymbol{x},t;\boldsymbol{\xi},\tau) = \Gamma_{pn}(\boldsymbol{\xi},\tau;\boldsymbol{x},t)\,. \tag{32}$$

Then

$$\Delta GP = -\int_{\infty}^{} d\tau \int_{\Sigma(\boldsymbol{\xi})} [u_i(\boldsymbol{\xi},\tau)] \upsilon_j c_{ijpq} \frac{\partial}{\partial \xi_q} \underline{\int_{\infty}^{} dt \int_{V(\boldsymbol{x})} f_n(\boldsymbol{x},t) \Gamma_{pn}(\boldsymbol{\xi},\tau;\boldsymbol{x},t)\, dV(\boldsymbol{x})\, d\Sigma(\boldsymbol{\xi})} \tag{33}$$

The underlined portion of Eq. (33) is recognized as the volumetric body force displacements. When these were assumed to be zero, the net change in the gravitational potential energy (ΔGP) was constrained to be zero. The seismic model was "ok" but the model was restricted to elastic rebound. Gravity had been inadvertently locked out of the energetics of the seismic process.

4 Conclusions

This paper is not "easy"; especially for those who are thoroughly versed and experienced in elastic rebound. Elastic rebound has historically been found to successfully explain and model almost all field observations and the few exceptions are easily classed as anomalies or problems for future study. To properly appreciate the gravity collapse seismic mechanism it is important to understand that most of the characteristics of elastic rebound are also characteristics of gravity collapse. Both mechanisms have a co-seismic change in elastic strain energy whose absolute magnitude equals the earthquake. Differences do exist but these may be subtle and hard to detect (see Appendix). It is also important to recognize that in the physical sciences a hypothesis

should be considered valid until it is shown to be inconsistent with either basic theory or observations.

There are only three parts to the gravity collapse mechanism; these are:

1. Tectonic stress originates from gravity acting on the Earth's topography and lateral density variations.
2. The intensity of the gravitational tectonic stress that results from the regional topographic features and lateral density variations that actually exist is comparable to the stress drops that characterize tectonic earthquakes.
3. The simplest seismic mechanism is to let the fault fail and slip in direct response to the gravitational tectonic stress.

Part #1 is taken directly from published literature; specific references are given in Sect. 1. Part #2 is based on mechanical analysis. Both gravitational tectonic stress and earthquake stress drops are in the range of tens of bar to several hundred bar. Part #3 is the only part of the gravity collapse mechanism that can be considered "new".

It is recognized that viscous deformation in some parts of the Earth can create locked-in elastic strain in other parts leading to the elastic rebound mechanism. But if the stress ultimately originates from gravity, the elastic rebound mechanism requires some form of mechanical isolation between the earthquake fault and the stress-causing topography or lateral density variations. From the perspective of gravitational tectonics, the gravity collapse mechanism is simpler than elastic rebound.

Appendix A

Elastic rebound and force-driven faulting

The similarities and distinctions between force-driven faulting and elastic rebound can be explored with a couple of plane-strain finite-element computer models. A plane strain model is a two-dimensional cross-section slice through a body that is much longer than it is tall or wide. Material properties, forces, and displacements are invariant along the length of the body; strain is limited to the plane of the cross section. Previous report Sects. 2.2.1 and 2.2.2 describe the conceptual models.

The finite-element model is a 200 by 200 km cross section of a much longer body. A 50-km-long, 200-m-wide area in the center of the model is the "fault zone". Figure A1 shows the arrangement of finite elements. Figure A2 shows the details of the fault zone. Material displacements are assumed to vary linearly between the vertices of each triangular element. The X and Y displacements of the vertices (nodes) are the unknowns in the models.

The boundary conditions are constant X or Y directed surface tractions applied to the sides of the model of force-driven faulting (Fig. A3) and fixed X or Y displacements of the nodes along the sides of the model of elastic rebound (Fig. A4). The fixed displacements and the surface tractions create a uniform initial shear stress of 100 bar throughout the material. This stress is exactly identical in both models.

Initially, the materials are homogeneous with a uniform Young's modulus of $E = 10^{12}$ dynes/cm^2. The corresponding shear modulus equals $E \div 2(1+\upsilon) = 4 \times 10^{11}$ dynes/cm^2, where $\upsilon = 0.25$ is Poisson's ratio. These problems are solved for the baseline displacements of the nodes (identical in both models).

To simulate faulting, the strength of the material in the fault zone (Young's modulus) is reduced to 1% of its initial value. The displacements attributable to faulting are the differences between the equilibrium displacements in the faulted or weakened models and the equilibrium displacements in the baseline models. Figure A5 shows the

displacements due to faulting in the force-driven model. Figure A6 shows the displacements due to faulting in the elastic rebound model. The dots are the nodal points located at the vertices of the triangular elements and the lines show the direction and relative magnitude of the nodal point displacements. Figure A7 shows the displacements along the sides of the fault zones; in this figure the width or thickness of the fault zones has been expanded to better display the displacement vectors. The maximum total displacement across the fault zone (slip) is 2.8 m.

The displacement fields are similar near the fault zones but they differ in the remainder of the models, Fig. A8 shows the difference between the displacement fields. For force-driven faulting there are displacements of the sides of the model that are locked out of the model of elastic rebound. These are the force-connected displacements that allow the forces to participate in the energetics of the faulting.

The energetics of these processes can be directly calculated. Stress and strain are constant within each triangular element so the elastic strain energy equals one-half the product of stress, strain, and the volume of the triangle. These were calculated and summed over the elements in the models. In the model of force-driven faulting, the work done by the forces is the scalar product of force and displacement, summed along the sides of the model. The net energetics and the shear stress in the fault zone are:

		Force-Driven Faulting	Elastic Rebound
Baseline Model	Total Strain Energy (ergs)	50×10^{22}	50×10^{22}
	Work Done by Forces (ergs)	100×10^{22}	***
	Shear Stress in the Fault Zone (bar)	100	100
Faulted Model	Total Strain Energy (ergs)	50.463×10^{22}	49.547×10^{22}
	Work Done by Forces (ergs)	100.927×10^{22}	***
	Shear Stress in the Fault Zone (bar)	55.2	53.9
Difference	Total Strain Energy (ergs)	$+0.463 \times 10^{22}$	-0.453×10^{22}
	Work Done by Forces (ergs)	$+0.927 \times 10^{22}$	***
	Stress Drop in the Fault Zone (bar)	44.8	46.1

For force-driven faulting, the model shows an *increase* in total elastic strain energy of $+0.463 \times 10^{22}$ ergs. This is one-half the additional work done by the forces (0.927×10^{22}). The excess energy less the strain energy in the part of the material that failed (Eq. 19) goes into the earthquake (seismic waves or work done in the fault zone). In the current model the energy in the failed material equals 0.011×10^{22} ergs so the energy available for the earthquake is 0.453×10^{22} ergs. For elastic rebound, the model shows a *decrease* in total elastic strain energy of -0.453×10^{22} ergs and there are no forces (hence there is no work done by the forces). The released elastic strain energy goes into the earthquake. The slip on the fault surface, the stress drop in the fault zone, and the energy available for the earthquake are similar in both models but the net energetics are starkly different. Also distinct are the displacements at long distances from the fault.

These energetics apply to a one-kilometer-thick slice of material. For an effective thickness of 15 km, the earthquake energy is $15 \times 0.453 \times 10^{22} = 6.795 \times 10^{22}$ ergs. If half this energy is converted into seismic waves, the corresponding surface wave magnitude is $M_s = 7.15$ (from $\log E = 11.8 + 1.5 \times M_s$ (Bolt, 2004, p. 339)).

The fault dimensions, fault slip, stress drop, and earthquake magnitude are consistent with the parameter ranges given in Kasahara (1981).

The initial stress in both baseline models was a uniform shear of 100 bar. The baseline pressure was zero. The stress change associated with faulting equals the stress distribution in the faulted model minus that in the baseline model. One display that shows this change is the intensity of the shear stress; where shear stress intensity equals one-half the difference between the maximum and minimum principal stress. Figure A9 shows the change in shear stress intensity associated with force-driven faulting. Figure A10 shows the change associated with elastic rebound. These maps show the stress drops associated with the two types of faulting; contours are at −64, −32, −16, −8, −4, −2, −1, 0, +1, +2, +4 bar. The maps are nearly but not quite identical. Figure A11 shows the difference between the change in shear stress intensity associated with force-driven faulting (Fig. A9) and that associated with elastic rebound

(Fig. A10). The contour interval on Fig. A11 is 0.5 bar.

Note: In force-driven faulting, the Coulomb stress represents a net stress increase. In elastic rebound, it represents a net stress decrease. A net stress increase would be consistent with an increased concentration of aftershocks.

Recall that the net force (i.e. surface traction) acting on the model of force-driven faulting is constant. Figure A11 shows the intensity of the shear stress distribution that is needed to balance that part of the net force that was acting on the fault before the fault failed. In general, the details of this stress will be dependent on the particular geomechanical system with most of the redistributed stress being shifted into the stiffer load-baring parts of the system. In the current model, the material outside the fault zone is homogeneous. In the Earth, the material strength is expected to be heterogeneous; the redistributed stress in the Earth is expected to be similarly heterogeneous. This redistributed stress is in addition to and distinct from the Coulomb stress (Fig. A10) that results from slip on the fault. It provides a possible explanation for earthquake-induced tectonic activity at long distances from the failed fault.

We should also note that the locked-in stress that is created by a force driven earthquake is anomalous. In viscoelastic materials, it is expected to viscously dissipate; this will re-establish the ambient force-induced stress on the fault. Post-seismic relaxation of the locked-in stress should be accompanied by post-seismic regional displacements.

This behavior may have been observed in the horizontal land surface displacements that accompanied the 10 December 1994 Sanriku-Haruka-Oki earthquake at the Japan Trench ($M = 7.6$). For this event, co-seismic and post seismic displacements were monitored with the Japanese Nationwide Permanent GPS Network (Heki and others, 1997). The co-seismic displacements were consistent with slip on a shallow interplate thrust fault. During the year following the earthquake, continuous post seismic displacements were observed. The direction and amplitude of these post seismic displacements was comparable with the co-seismic displacements and they developed at an exponentially decreasing rate, consistent with viscous relaxation of a locked-in elastic stress.

References

Aki, K. and Richards, P. G.: Quantitative Seismology, W. H. Freeman, New York, 1980.

Artyushkov, E. V.: Stresses in the lithosphere caused by crustal thickness inhomogenities, J. Geophys. Res., 78, 7675–7708, 1973.

Barrows, L.: The Effects of Locked-in Pressure on the Mechanics of Faulting, Seismol. Res. Lett., 79, 4, 544–545, 2008.

Barrows, L. and Langer, C. J.: Gravitational potential as a source of earthquake energy, Tectonophysics, 76, 237–255, 1981.

Barrows, L. J. and Paul, K. M.: A finite-element modeling approach to gravitational tectonic stress and earthquakes, J. Geoscience Education, NAGT, Bellingham, Washington, 46, 1–17, 1998.

Bolt, B. A.: Earthquakes, W. H. Freeman, New York, 2004.

DeJong, K. A. and Scholten, R. (Eds.): Gravity and Tectonics, John Wiley and Sons, New York, 1973.

Desai, C. S. and Abel, J. F.: Introduction to the Finite Element Method, Van Norstrand & Reinhold, New York, 1972.

Dickinson, W. R.: Tectono-Stratigraphic Evolution of Subduction-Controlled Sedimentary Assemblages, in: Island Arcs, Deep Sea Trenches and Back-Arc Basins, edited by: Talwani, M. and Pitman III, W. C., Am. Geophys. Union, Washington, D.C., 33–40, 1977.

Hamilton, W.: Tectonics of the Indoneasean Region, Geol. Soc. Malaysia Bull., 6, 3–10, 1973.

Heki, Kosuke, Shin'ichi Miyazaki, and Hiromichi Tsuji: Silent fault slip following an interplate thrust earthquake at the Japan Trench, Nature, 386, 595–598, 1997.

Hough, S. E.: Earthshaking Science, Princeton University Press, Princeton, N.J., 238 pp., 2002.

Jacoby, W. R.: Instability in the upper mantle and global plate movements, J. Geophys. Res., 75, 5671–5680, 1970.

Kasahara, K.: Earthquake Mechanics, Cambridge University Press, Cambridge, 1981.

Kellogg, O. D.: Foundations of Potential Theory, Dover Publications, New York, 1953.

Plafker, G.: Alaskan Earthquake of 1964 and the Chilean Earthquake of 1960 – Implication for Arc Tectonics, J. Geophys. Res., 77, 901–925, 1972.

Press, F. and Jackson, D.: Vertical Extent of Faulting and Elastic Strain Energy Release, in: The Great Alaska Earthquake of 1964 – Seismology and Geodesy, National Academy of

Sciences, Washington, D.C., p. 110, 1972.

Ramberg, H.: Gravity, Deformation, and the Earth's Crust, Academic Press, London, 1981.

Reid, H. F.: The Mechanics of the Earthquake, in: The California Earthquake of April 18, 1906, Report of the State Investigation Commission, Vol. 2, Garnegie Institute of Washington, Washington, D.C., 16–28, 1910.

Ruff, L. J.: State of Stress Within the Earth, in: The International Handbook of Earthquake and Engineering Seismology, Academic Press, London, 539–557, 2002.

Stein, S. and Wysession, M.: An Introduction to Seismology, Earthquakes, and Earth Structure, Blackwell Publishing, Malden, MA, 498 pp., 2003.

Zienkiewicz, O. C.: The Finite Element Method in Engineering Science, McGraw-Hill, London, 1971.

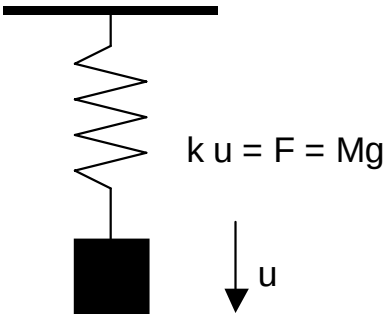

Fig. 1. Simple spring-mass oscillator.

Reducing the spring constant:

- lowers the gravitational potential energy,
- increases the elastic strain energy, and
- causes the mass to oscillate about its new equilibrium position.

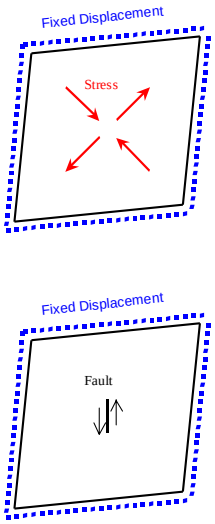

Fig. 2. Conceptual model, elastic rebound.

– Elastic Strain Energy ⇒ Earthquake Energy

(a) A block of elastic material enclosed in a rigid frame. Distort the frame creating locked-in stress and strain within the material. This is shown as the maximum and minimum principal stresses associated with a simple shear deformation. **(b)** Let a fault fail and slip in direct response to the stress. Elastic strain energy is transformed into the earthquake. The change in locked-in elastic stress drives slip on the fault. The mechanics are those of the elastic rebound mechanism.

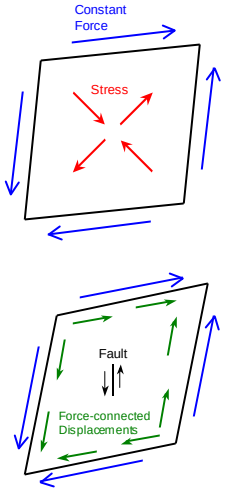

Fig. 3. Conceptual model, force-driven faulting.

$$\text{Work} \Rightarrow \begin{cases} +\text{Elastic Strain Energy} \\ = \\ \text{Earthquake Energy} \end{cases}$$

(a) The same block of elastic material loaded by constant forces. The forces create stress and strain within the material. **(b)** Let a fault fail and slip in direct response to the stress. When the fault fails the block temporarily becomes less rigid so there is further deformation of the block (shown by the solid-head arrows). Force times displacement equals work or energy. Half of this energy is transformed into the earthquake and half goes into an increase in locked-in elastic strain. The mechanics are those of the gravity collapse mechanism.

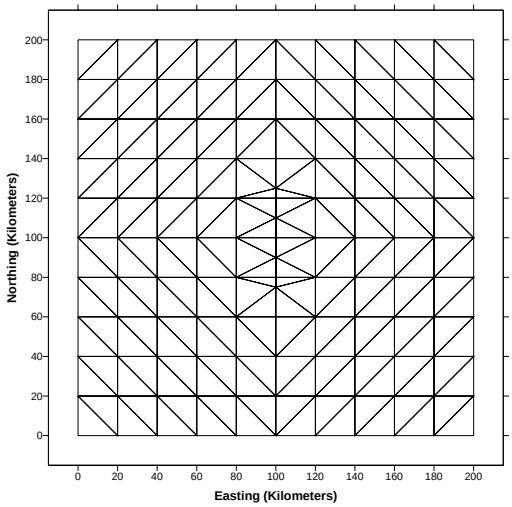

Fig. A1. Plane strain finite element model.

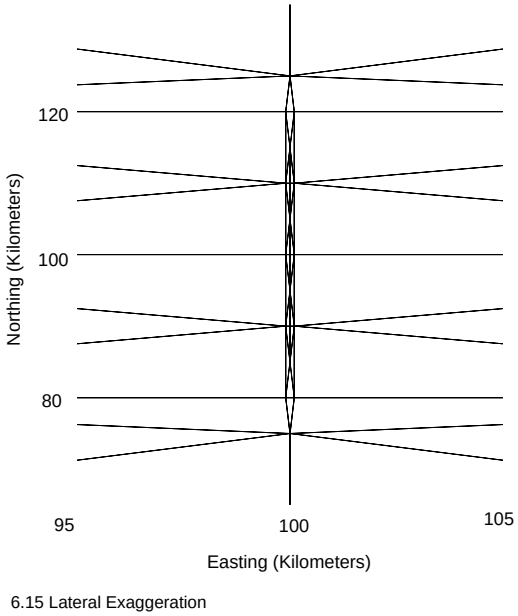

Fig. A2. Detail of modeled fault zone.

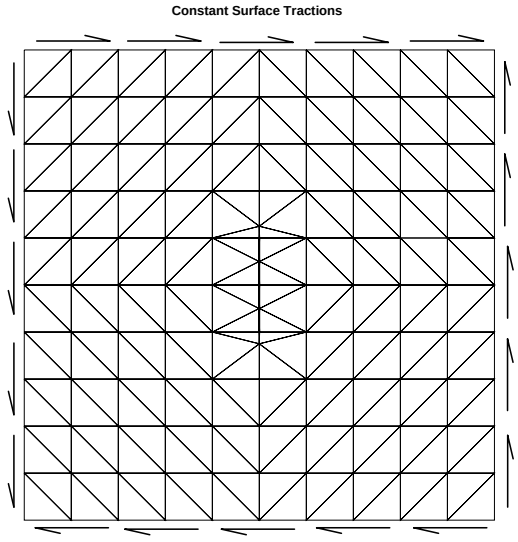

Fig. A3. Boundary conditions, force-driven faulting.

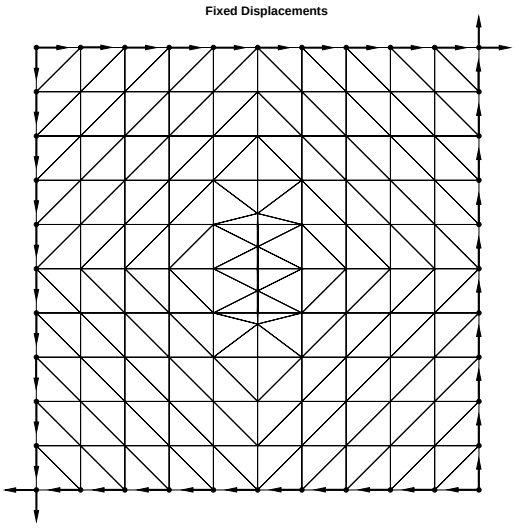

Fig. A4. Boundary conditions, elastic rebound

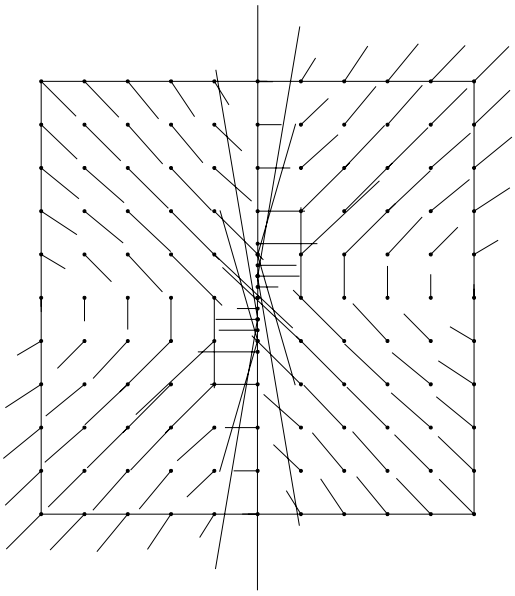

Fig. A5. Nodal point displacements, force-driven faulting.

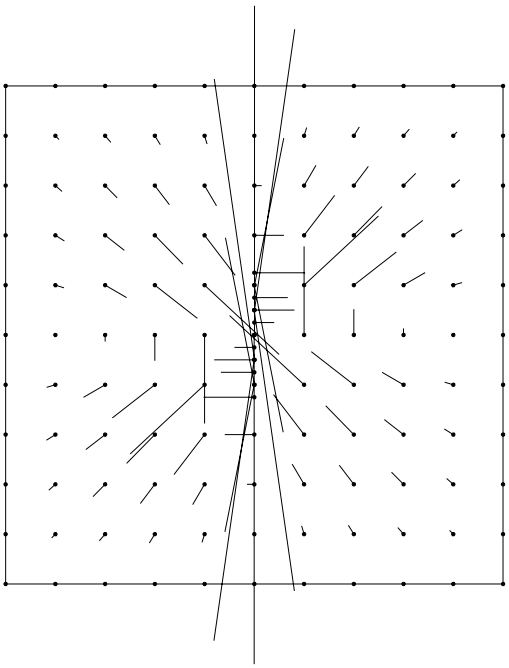

Fig. A6. Nodal point displacements, elastic rebound.

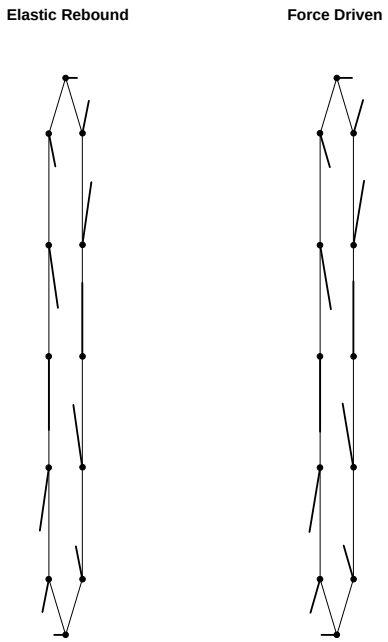

Fig. A7. Comparison of fault zone displacements.

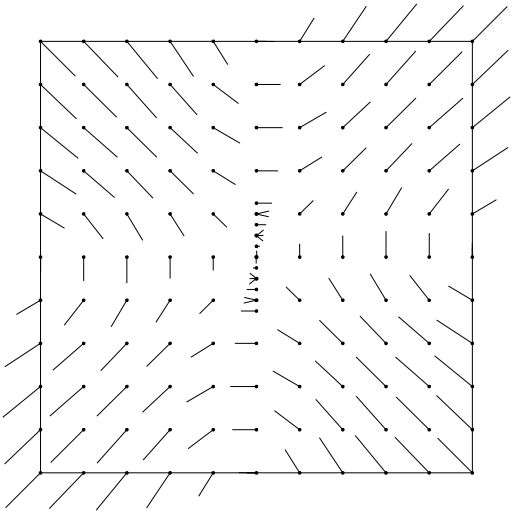

Fig. A8. Displacement differences, force-driven minus elastic rebound.

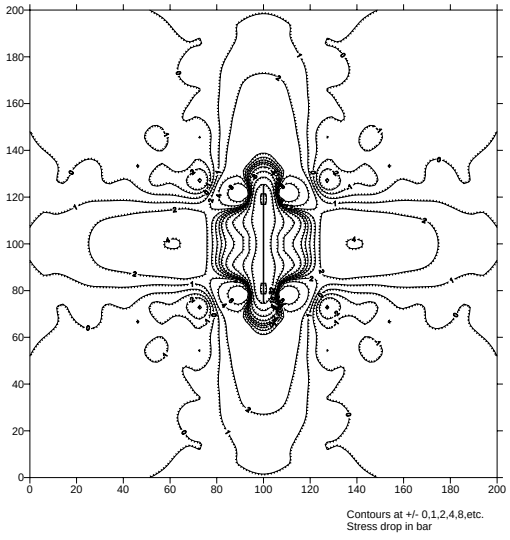

Fig. A9. Drop in shear stress intensity, force-driven faulting.

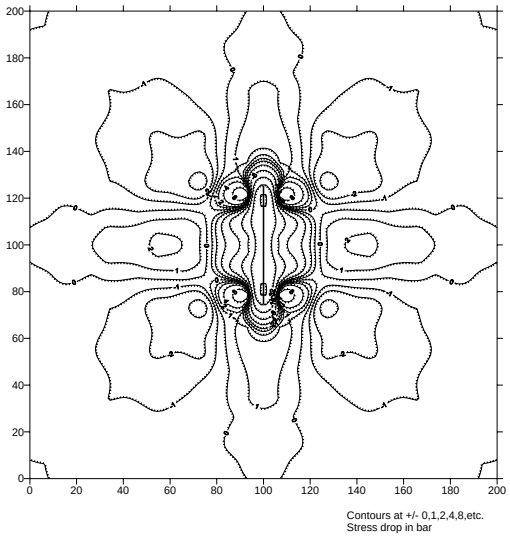

Fig. A10. Drop in shear stress intensity, elastic rebound.

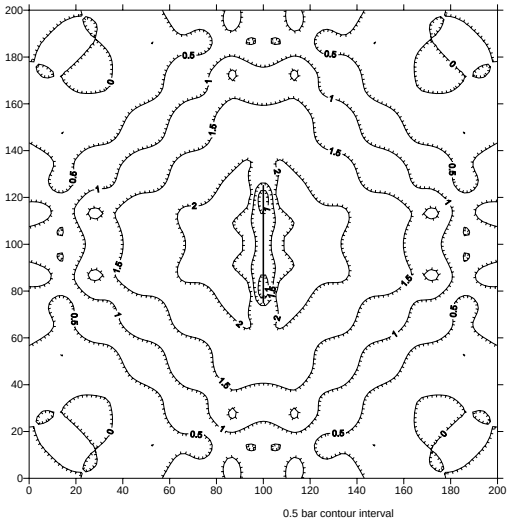

Fig. A11. Shear stress intensity differences, force-driven faulting minus elastic rebound